Current Microbiology (2025) 82:282
https://doi.org/10.1007/s00284-025-04246-6

Co-variation of Host Gene Expression and Gut Microbiome in Intestine-Specific *Spp*1 Conditional Knockout Mice

Na Li[1] · Guangqi Gao[1] · Tao Zhang[1] · Chunyan Zhao[1] · Yue Zhao[1] · Yong Zhang[2] · Zhihong Sun[1]

Received: 6 November 2024 / Accepted: 14 April 2025

Abstract

Osteopontin, which is a highly phosphorylated and glycosylated acidic secreted protein encoded by the secreted phosphoprotein 1 (*Spp*1) gene, plays a crucial role in immune regulation, inflammatory responses, and cell adhesion. However, its impact on intestinal gene expression and gut microbiota remains underexplored. In this study, we developed an *Spp*1 conditional knockout mouse model to investigate alterations in the intestinal transcriptome and microbiome, with particular emphasis on changes in gene expression and predicted metabolic pathways. Our findings demonstrated that *Spp*1 gene conditional knockout significantly modified the expression of genes involved in immune regulation and lipid metabolism. Moreover, metagenomic analysis revealed marked shifts in gut microbial diversity and predicted the metabolic pathways associated with digestion, absorption, and lipid metabolism. These results suggest that *Spp*1 is instrumental in maintaining gut microbial equilibrium and in regulating host lipid metabolism and immune responses. This study offers new insights into the role of *Spp*1 in host–microbiota interactions and the potential foundations for developing related therapeutic strategies.

Introduction

Osteopontin (OPN), a highly phosphorylated and glycosylated acidic secretory protein, encompasses an Arg-Gly-Asp (RGD) integrin-binding sequence, a concealed integrin-binding domain, and a CD44 binding site [1]. Initially identified in osteoblasts, OPN results from the expression of the secreted phosphoprotein 1 (*Spp*1) gene [2]. Its expression extends to osteocytes, epithelial cells, neurons, lymphocytes, and macrophages and is widely distributed in tissues, including the bone, brain, kidney, and intestine [3]. OPN has vital functions in mammalian organisms, including bone formation, immune regulation, cell migration, inflammatory responses, tissue repair, and modulation of cellular functions [4, 5]. There are two primary forms of OPN: secreted osteopontin (sOPN) and intracellular osteopontin (iOPN). In intestinal tissues, various cell types, such as intestinal epithelial cells and activated T lymphocytes, secrete sOPN, which primarily facilitates cell adhesion, migration, and immune regulation [1]. In contrast, iOPN is retained within cells such as macrophages and dendritic cells, where it contributes to intracellular signaling, immune responses, and cell regulation without being secreted extracellularly [6, 7]. Studies have demonstrated that OPN modulates intestinal immune cell activity and cytokine secretion, thereby maintaining the immune equilibrium and responses in the gut. Additionally, OPN influences gut microbiota composition and function, as well as its metabolites, mitigating intestinal inflammation and safeguarding the gut against injury [8–10]. Thus, OPN not only plays a pivotal role in immune system regulation and gut health maintenance but may also perform more intricate biological functions through its interactions with the gut microbiota. Recent investigations have suggested that OPN could be instrumental in modulating the composition and functionality of the gut microbiota, potentially through mechanisms that directly affect microbial populations or indirectly influence the microbiome by altering the intestinal microenvironment and immune responses [11].

✉ Na Li
18004899551@163.com

✉ Guangqi Gao
guangqigao@163.com

✉ Yong Zhang

✉ Zhihong Sun

[1] Key Laboratory of Dairy Biotechnology and Engineering (IMAU), Ministry of Education, Inner Mongolia Agricultural University, Hohhot, People's Republic of China

[2] The Fourth Medical Center of PLA General Hospital, No. 51 Fucheng Road, Haidian District, Beijing 100037, China

Published online: 06 May 2025

This study used an intestine-specific *Spp*1 conditional knockout mouse model to investigate how OPN deficiency affects gut gene expression and microbiota composition. The primary objective of this study was to elucidate the impact of OPN deficiency on gene expression and the gut microecosystem and to analyze the potential correlation between these two factors. This research not only contributes to the understanding of the biological function of OPN within the gut, but also illuminates the intricate interactions between the gut microbiota and host gene regulation, providing novel insights and theoretical foundations for future research into the mechanisms underlying intestinal diseases.

Materials and Methods

Experimental Animals

This study utilized specific pathogen-free (SPF) C57BL/6 mice with intestine-specific conditional knockout of the *Spp*1 gene ($Spp1^{[flox/flox,\ Vil1-cre]}$). An animal model was established by crossing male $Spp1^{[flox/flox]}$ mice with female $Spp1^{[flox/flox;\ Vil1-cre]}$ mice. In the $Spp1^{[flox/flox]}$ genotype, LoxP sites flank the *Spp*1 gene, whereas the $Spp1^{[Vil1-Cre]}$ genotype expresses Cre recombinase specifically in the intestinal epithelium. Offspring were genotyped, and those exhibiting intestine-specific OPN deficient were designated as the CKO (conditional knockout) group ($n = 3$), whereas their wild-type littermates served as the wild-type (WT) control group ($n = 3$). All animals were housed in an SPF-grade facility under controlled environmental conditions: a 12 h/12 h light–dark cycle, a temperature of 22 ± 2 °C, and a humidity of 50 ± 10%. Food and water were provided ad libitum throughout the study. The mice were monitored daily and euthanized at the end of the study period at 2 months of age. Colonic content and tissues were collected for metagenomic and transcriptomic sequencing, and additional colon samples were collected for histopathological analysis. This study was performed in strict compliance with the GB/T35823-2018 guidelines for animal research and strictly adhered to ethical standards. This study was approved by the Animal Welfare and Ethics Committee of Beijing Huafukang Bioscience Co., Ltd. (approval number: HFK-AP-20230523).

Mouse Genotyping

Genomic DNA was extracted from mouse tail tissue using an EasyPure® Genomic DNA Kit with RNase A (TransGen Biotech, Beijing, China). Two primer sets were used for polymerase chain reaction (PCR) amplification: set 1 (F1:5'-GTAGAGCGTCATTGCAGTTTCAT-3'and R1:5'-TTATTGTAGTTGAGCACCCATGTTC-3') and set 2 (Vil1-cre-F:5'-CCATAGGAAGCCAGTTTCCCTTC-3'and Vil1-cre-R:5'-TTCCAGGTATGCTCAGAAAACGC-3'). The presence of target bands at 207 bp for primer set 1 and 304 bp for primer set 2 in PCR products indicated homozygous knockout status for $Spp1^{[flox/flox,Vil1-cre]}$.

Histological Analysis

Mouse colon tissues were fixed in paraformaldehyde, embedded in paraffin, and sectioned. Subsequently, Alcian Blue-Periodic Acid-Schiff (AB-PAS) staining was performed on the tissue sections (n = 3). Mucin and polysaccharide distributions were observed using a 3DHISTECH P250 FLASH panoramic scanner (3DHISTECH, Hungary).

Transcriptomic Analysis

Colon tissue samples weighing 100 mg were collected from WT and CKO mice ($n = 3$), immediately flash-frozen in liquid nitrogen, and stored at −80°C for subsequent RNA-seq analysis. Total RNA was extracted using an Agilent 2100 Bioanalyzer RNA 6000 Nano Kit (catalog number 5067–1511, Agilent Technologies, USA). Following quality control, paired-end sequencing (PE150) was performed on an Illumina Novaseq X Plus platform using the Mus musculus genome (GRCm39) for gene annotation [12]. Differential gene expression analysis was performed using DESeq (v1.38.3), with a threshold for differentially expressed genes set at $|\log_2$ Fold Change$| > 1$ and $p < 0.05$.

Gene Ontology (GO) enrichment analysis was carried out using topGO (v2.50.0). The hypergeometric distribution method was applied to calculate p-values, with significant enrichment defined as $p < 0.05$, to identify the significantly enriched GO terms and determine the primary biological functions of the differentially expressed genes. To investigate pathway-level changes, the Kyoto Encyclopedia of Genes and Genomes (KEGG) pathway enrichment analysis was conducted using clusterProfiler (v4.6.0), with pathways considered to be significantly enriched at $p < 0.05$. Gene Set Enrichment Analysis (GSEA, v4.1.0) was employed to further explore relevant gene sets.

Metagenomic Sequencing

At the end of the experiment, approximately 100 mg of colon fecal samples from each mouse were used for metagenomic sequencing ($n = 3$). Total DNA was extracted from colonic fecal samples using a QIAamp DNA Stool Mini Kit (QIAGEN, Hilden, Germany). Sequencing libraries were prepared using the NEBNext Ultra DNA Library Preparation Kit (New England Biolabs Inc., Ipswich, MA, USA). The Illumina HiSeq 2500 sequencing platform generated raw data, which

were subsequently processed using Kneaddata software (http://huttenhower.sph.harvard.edu/kneaddata) to remove low-quality and host-contaminated reads. The resulting data were subjected to species annotation and functional analysis using the Kraken2 and HUMAnN2, respectively [13].

Statistical Analysis

All experimental data were reported as mean ± standard deviation (SD). Transcriptomic analysis and metagenomic sequencing statistical analyses were conducted using the R (v4.1.1), and the Wilcoxon test was used to assess the differences between the two groups (without FDR correction). Statistical significance was set at $p < 0.05$. Graphical representations were generated using GraphPad Prism 9.5, along with R packages and STAMP software (v2.1.3). In the Spearman correlation analysis, threshold values were set to $p < 0.05$, |rho|> 0.4, and multiple corrections were performed using Benjamini Hochberg FDR.

Result

Knockout of the *Spp*1 Gene Leads to a Reduction in the Colonic Mucus Layer in Mice

AB-PAS staining was used to visualize mucus distribution and integrity to evaluate alterations in the colonic mucus layer and its composition in mice. The findings revealed that colon sections from WT mice (WT group) exhibited a reddish-purple hue following AB-PAS staining (Fig. 1), indicative of positive PAS staining and abundant acidic mucus, which was predominantly secreted by goblet cells and distributed uniformly along the epithelial cell surface at a healthy thickness. In contrast, *Spp*1 gene intestine-specific conditional knockout mice (CKO group) exhibited a markedly reduced colonic mucus layer and diminished staining intensity (Fig. 1), suggesting an impairment in both the number and function of goblet cells. These findings demonstrated that OPN is essential for preserving the structure and function of the intestinal mucus layer. The observed reduction in the mucus layer in CKO mice likely

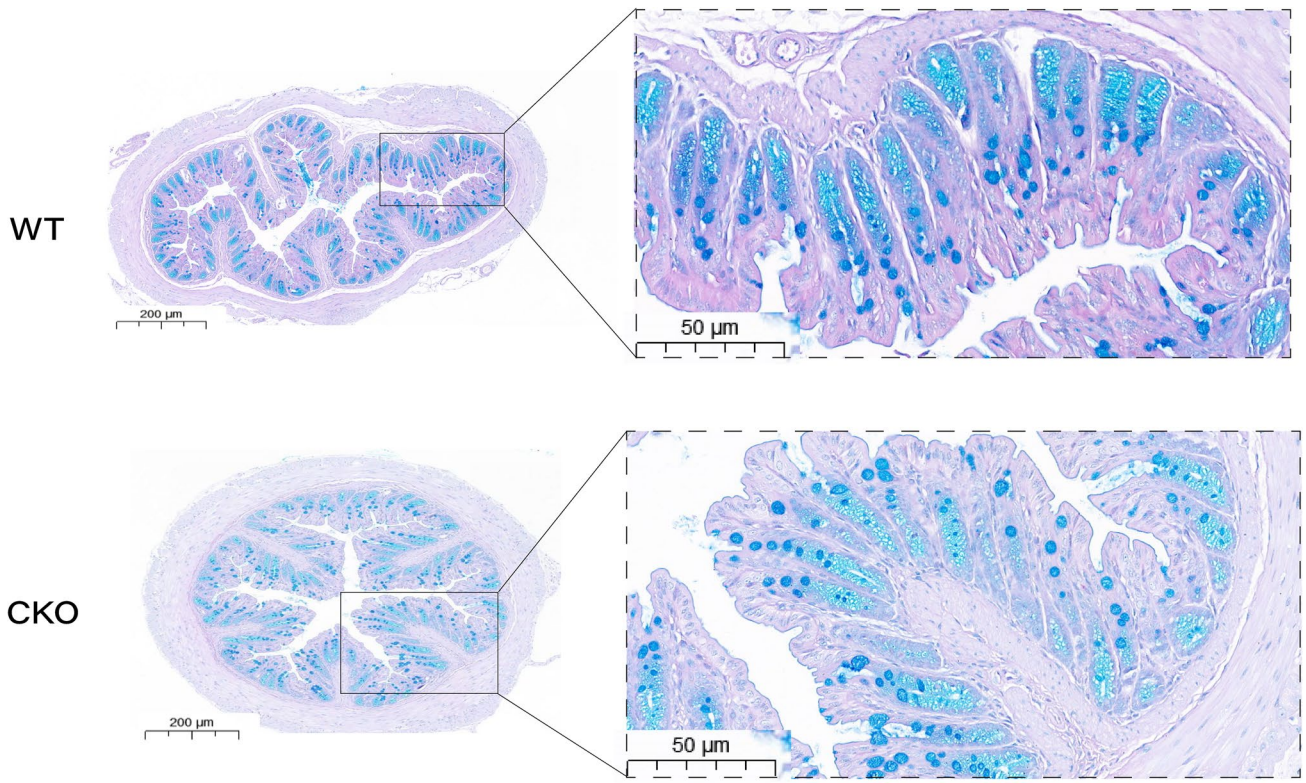

Fig. 1 Representative micrographs of Alcian Blue-Periodic Acid-Schiff (AB-PAS)-stained colon tissue sections. WT represents wild-type mouse colon sections stained with AB-PAS, whereas CKO represents colon sections from intestinal epithelial-specific OPN-deficient mice stained with AB-PAS. The color intensity indicates the amount of mucin secreted; the darker the color, the higher the amount of mucin secreted

compromises the intestinal barrier, potentially increasing susceptibility to infections and inflammation.

Gene Expression Pattern Changes in the Colon Tissues of *Spp*1 Conditional Knockout Mice

To investigate the effects of OPN deficiency on gene expression in colon tissues, transcriptomic sequencing was performed on colonic samples. Analysis of the sequencing data against the reference genome yielded annotations for 21,959 expressed genes. A comparison between WT and CKO mice revealed significant differences in the expression of 169 genes in the colonic tissues of CKO mice ($p < 0.05$, $|\log_2 \text{Fold Change}| > 1$). Of these, 115 genes were upregulated and 54 were downregulated in the CKO group (Fig. 2a and b, Table S1). These findings suggest that the absence of OPN-encoding genes induces modifications in the gene expression profiles of colon tissues.

To ascertain the functional implications of these differentially expressed genes, GO functional enrichment and KEGG analyses were performed. GO analysis revealed that the differentially expressed genes were predominantly associated with processes such as cell adhesion (GO:0007155), biological adhesion (GO:0022610), acute inflammatory response (GO:0002526), extracellular matrix organization (GO:0030198), extracellular space (GO:0005615), cell surface (GO:0009986), extracellular structure organization (GO:0043062), cell–cell signaling (GO:0007267), and multicellular organism development (GO:0007275) ($p < 0.05$, Fig. 2c). Furthermore, KEGG enrichment analysis revealed that differentially expressed genes in CKO mice relative to the WT group were notably linked to immune and metabolic functions. The implicated pathways involved

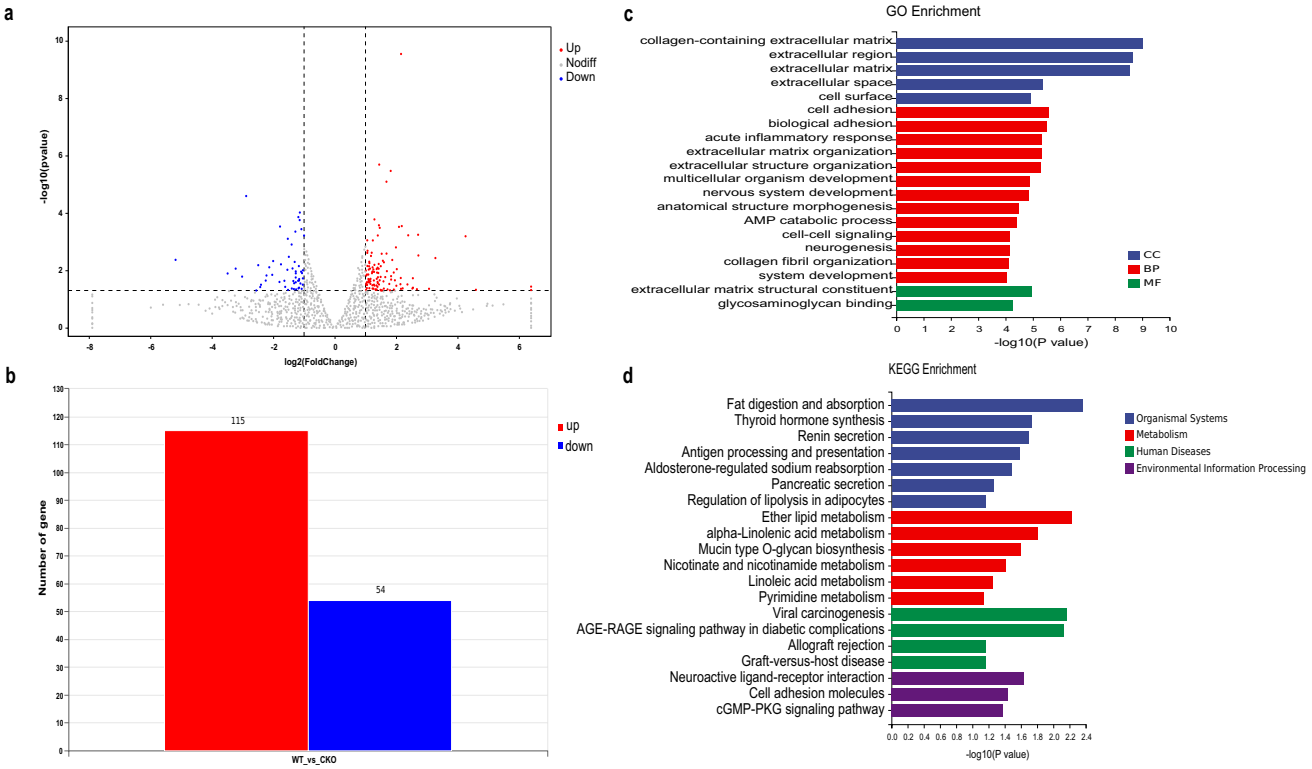

Fig. 2 CKO-induced differential gene expression and functional enrichment in the gut. **a** Volcano plot of differentially expressed genes in the gut of CKO mice. The x-axis represents $\log_2$ Fold Change, and the y-axis represents the negative $\log_{10}$ of the significance level. The two vertical dashed lines represent the thresholds for fold change in gene expression, and the horizontal dashed line represents the significance threshold. Red dots represent significantly upregulated genes ($\log_2$ Fold Change ≥ 1 and $p < 0.05$), blue dots represent significantly downregulated genes ($\log_2$ Fold Change ≤ -1 and $p < 0.05$), and gray dots represent genes with no significant differences. **b** Changes in differentially expressed genes in the gut of CKO mice. In **b**, the x-axis shows the comparison groups used for differential analysis and the y-axis represents the number of differentially expressed genes. Red indicates the total number of upregulated genes in the CKO group, whereas blue indicates the total number of downregulated genes. **c** GO functional enrichment of differentially expressed genes in the gut of CKO mice: the x-axis represents the GO terms and the y-axis represents the $-\log_{10}$ (p-value) of GO term enrichment. Different colors indicate the KEGG categories: Cellular Component (CC), Biological Process (BP), and Molecular Function (MF). **d** KEGG functional enrichment of differentially expressed genes in the gut of CKO mice; the x-axis represents the pathways and the y-axis represents the $-\log_{10}$ (p-value) of pathway enrichment. Blue, organismal systems; red, metabolism; green, human diseases; and purple, environmental information processing

encompassed fat digestion and absorption (Pathway ID: mmu04975), antigen processing and presentation (Pathway ID: mmu04612), regulation of lipolysis in adipocytes (Pathway ID: mmu04923), ether lipid metabolism (Pathway ID: mmu00565), alpha-linolenic acid metabolism (Pathway ID: mmu00592), mucin type O-glycan biosynthesis (Pathway ID: mmu00512), nicotinate and nicotinamide metabolism (Pathway ID: mmu00760), linoleic acid metabolism (Pathway ID: mmu00591), pyrimidine metabolism (Pathway ID: mmu00240), cell adhesion molecules (Pathway ID: mmu04514), and the cGMP-PKG signaling pathway (Pathway ID: mmu04022). Notably, pathways with strong connections to immune responses included antigen processing and presentation, mucin O-glycan biosynthesis, cell adhesion, and the cGMP-PKG signaling pathway ($p < 0.05$, Fig. 2d).

The investigation revealed that *Spp*1 gene deletion-induced alterations in colon tissue resulted in compromised digestive absorption, lipid metabolism, and immune response functions. Specifically, genes related to inflammation and signaling, including *C*3 (Complement Component 3), *Adora*1, and *Cdh*3, were markedly upregulated in the CKO group, while those associated with lipid metabolism and cell adhesion, such as *Pla2 g12b*, glucosaminyl (N-acetyl) transferase 3 (*Gcnt*3), and *Adra2a*, were significantly downregulated (Table 1). Intestine-specific conditional Knockout of the OPN gene modified intestinal gene expression patterns, particularly affecting lipid metabolism and intercellular adhesion. These alterations potentially contribute to functional disruptions in colon tissues, impacting the immune response and barrier functions, thus increasing the risk of colitis and other intestinal disorders.

Based on these observations, we can infer that OPN expression in colon tissues substantially influences the development of intestinal diseases in mice, as well as the signaling, cell adhesion, and lipid metabolism processes. This influence may operate through two mechanisms: First, endogenous OPN modulates gut-associated gene expression, and second, OPN may affect the intestinal symbiotic microbiota, thereby indirectly affecting intestinal health. To further investigate this mechanism, metagenomic sequencing was used to conduct a comprehensive analysis of the gut microbiota in the two groups.

Effects of *Spp*1 Gene Conditional Knockout on the Structure and Composition of Gut Microbiota in Mice

Analysis of microbial diversity revealed no significant differences in Shannon and Simpson indices between the two mouse groups; however, the CKO group exhibited a trend toward increased α-diversity compared to the control group (Fig. 3a). Additionally, Bray-Curtis distance analysis indicated a notable divergence in the gut microbiota structure between the CKO and control groups, suggesting potential structural differences in the microbial composition (Fig. 3b). Further examination of the gut microbiota species composition identified 15 components (Fig. 3c, Table S2), including various bacterial species such as *Akkermansia muciniphila*, *Duncaniella dubosii*, *Muribaculum gordoncarteri*, *Paramuribaculum intestinale*, *Ligilactobacillus murinus*, and *Duncaniella* sp. C9, *Muribaculum intestinale*, *Bacteroides caecimuris*, *Duncaniella* spp. B8, *Blautia pseudococcoides*, *Phocaeicola vulgatus*, *Bacteroides faecium*, *Bacteroides uniformis*, *Parabacteroides distasonis,* and *Bacteroides caccae* (Fig. 3e). Among these, *A. muciniphila* is normally a notable member of the gut flora, but its abundance was significantly reduced in the OPN-CKO mice relative to WT ($p < 0.05$) (Fig. 3d).

Alterations in the gut microbiota may induce changes in intestinal metabolic pathways. Annotation of gut functions using HUMAnN2 software identified 274 metabolic pathways within the microbiota of all mice, with 25 pathways showing significant differences between groups ($p < 0.05$) (Fig. 4, Table S3). Notably, eight of these differential pathways were related to fatty acid biosynthesis and metabolism, including stearic acid biosynthesis, saturated fatty acid elongation, oleic acid biosynthesis

Table 1 Candidate gene screened by transcriptome analysis between WT and CKO mice

Gene	Description	Expression pattern in CKO
*C*3	*C*3 protein is a complement protein that regulates inflammation	UP
*Cdh*3	Members of the cadherin family exhibit abnormal regulation in various cancers	UP
*Adora*1	*ADORA*1 is an adenosine receptor closely associated with early Parkinson's disease and cognitive impairment	UP
Pla2 g12b	It is a member of phospholipase A2, crucial for cell signaling, inflammation, and lipid metabolism	Down
*Gcnt*3	This gene activates β−1,6-N-acetylglucosamine transferase activity for O-glycosylated glycoproteins	Down
Adra2a	This gene activates adrenergic receptor activity and regulates synaptic vesicle exocytosis	Down

"Gene" refers to the genes selected from the differentially expressed genes, "Description" provides a description of the gene, and "Expression pattern in CKO" indicates the expression pattern of the gene in the CKO group

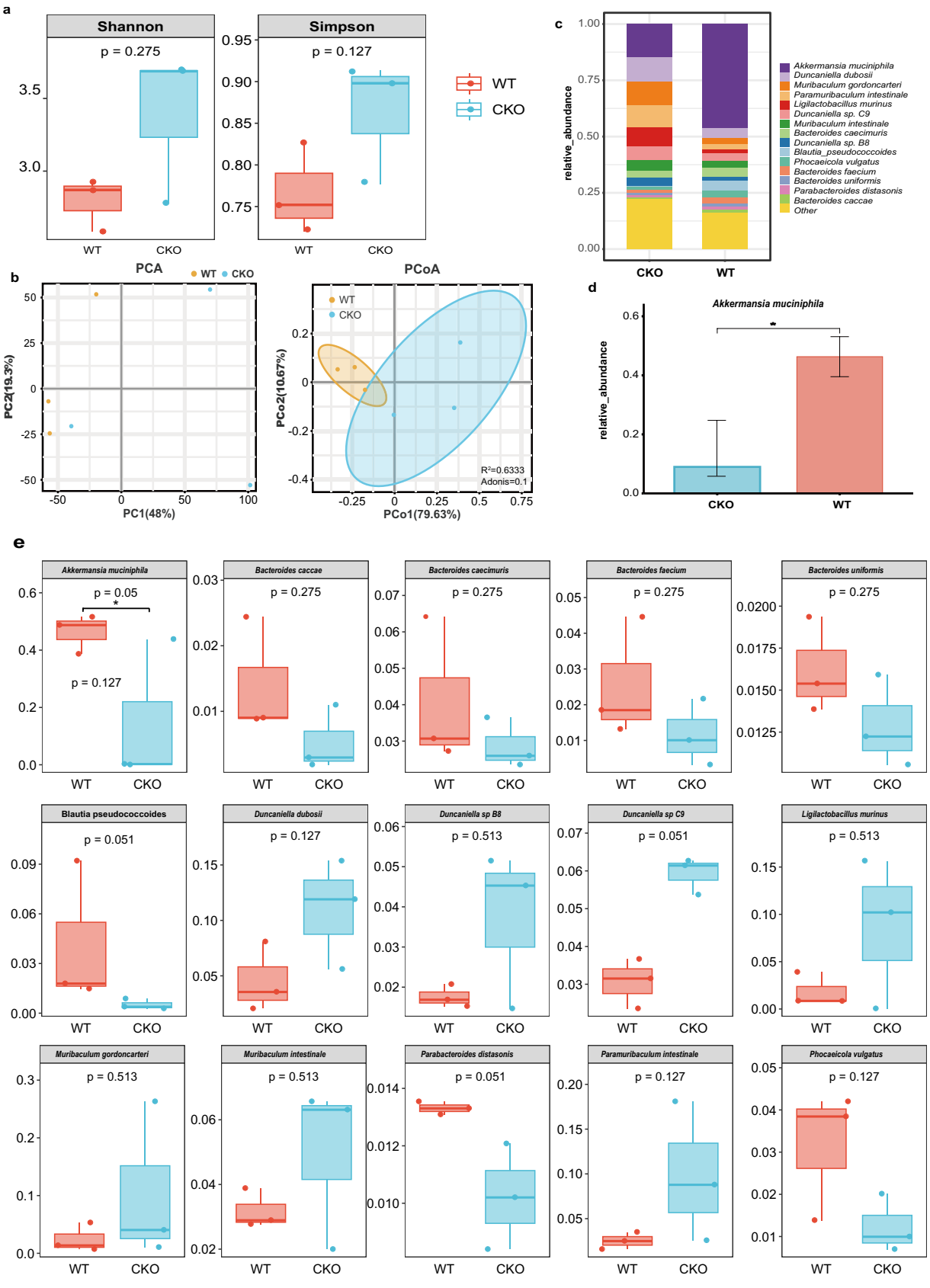
a
Shannon
p = 0.275
Simpson
p = 0.127
WT
CKO
b
PCA
PC2(19.3%)
PC1(48%)
PCoA
PCo2(10.67%)
PCo1(79.63%)
R²=0.6333
Adonis=0.1
c
relative_abundance
Akkermansia muciniphila
Duncaniella dubosii
Muribaculum gordoncarteri
Paramuribaculum intestinale
Ligilactobacillus murinus
Duncaniella sp. C9
Muribaculum intestinale
Bacteroides caecimuris
Duncaniella sp. B8
Blautia_pseudococcoides
Phocaeicola vulgatus
Bacteroides faecium
Bacteroides uniformis
Parabacteroides distasonis
Bacteroides caccae
Other
d
Akkermansia muciniphila
relative_abundance
e
Akkermansia muciniphila
p = 0.05
p = 0.127
Bacteroides caccae
p = 0.275
Bacteroides caecimuris
p = 0.275
Bacteroides faecium
p = 0.275
Bacteroides uniformis
p = 0.275
Blautia pseudococcoides
p = 0.051
Duncaniella dubosii
p = 0.127
Duncaniella sp B8
p = 0.513
Duncaniella sp C9
p = 0.051
Ligilactobacillus murinus
p = 0.513
Muribaculum gordoncarteri
p = 0.513
Muribaculum intestinale
p = 0.513
Parabacteroides distasonis
p = 0.051
Paramuribaculum intestinale
p = 0.127
Phocaeicola vulgatus
p = 0.127

◂**Fig. 3** The microbial diversity and species-level map of the CKO mouse gut microbiota. **a** Changes in the Shannon index and Simpson index of the gut microbiota between the two groups (n = 3): The box plot in **a** shows the interquartile range of the values for each group. The line inside the box represents the median, and the dashed lines indicate the minimum and maximum values within 1.5 times the interquartile range. The points above or below the upper and lower lines are outliers. **b** Changes in gut β-diversity, PCA, and PCoA between the two groups. The symbols representing the samples from the two groups are shown in different colors, and the results of the Adonis test are displayed in the bottom-right corner of the PCoA plot. **c** Changes in the gut microbiota structure between the two groups of mice. In **c**, the species with significantly different abundances between the two groups are shown, with different colors representing different species. **d** Changes in the abundance of *Akkermansia muciniphila* in the gut between the two groups of mice; the y-axis represents species abundance, and the x-axis represents the groups (*: $p < 0.05$). **e** Bar plot of the species composition and abundance of the gut microbiota between the two groups; the y-axis represents species abundance, and the x-axis represents the groups. Statistical significance was assessed using a two-sided Wilcoxon rank-sum test, with $p < 0.05$ considered statistically significant

IV (anaerobic), palmitic acid biosynthesis I (from (5Z)-dodecenoic acid), (5Z)-dodecenoic acid biosynthesis, cerotic acid biosynthesis, cis-vaccenic acid biosynthesis, and the super fatty acid biosynthesis pathway initiated by *Escherichia coli*. Additionally, functional differences in the gut microbiota involved pathways associated with glycolysis, amino acid biosynthesis, nucleotide and phospholipid biosynthesis, and vitamin and cofactor biosynthesis. These findings suggest that OPN may act as a signaling molecule, indirectly regulating host metabolic and physiological states through its influence on gut microbiota structure and function.

Notably, the observed differences in gut microbiota functions between CKO and WT mice were closely related to digestive absorption, lipid metabolism, and synthesis functions, aligning with the functional alterations detected in the transcriptomic profiles of colon tissues. These findings underscore the multifaceted role of OPN in gut function regulation, including its direct effects on host cell activity and indirect effects on host metabolism through the gut microbiota. Moreover, the observed host-microbial compositional changes exhibited synergistic interactions.

Coordinated Changes in Gene Expression and Compositional Microbiota of Mouse Gut Tissue Induced by *Spp*1 Gene Conditional Knockout

The investigation revealed that modifications in the expression of the OPN-encoding gene (*Spp*1) exerted both direct effects on host cell functions and potential alterations to the gut environment, consequently affecting the composition and function of the gut microbiota. These findings highlight the intricate interactions between host genes and the gut microorganisms. To elucidate the relationship between gut microbes and host gene expression, researchers conducted Spearman correlation analysis to quantify the associations between the relative abundances of gut microbes and differentially expressed genes in mouse colon tissues. As shown in Fig. 5a, C3 and *Abi3bp* were positively correlated with *Pusillibacter faecalis*, whereas *Gcnt*3 was negatively correlated with *Duncaniella dubosii*. *Alistipes indistinctus* exhibited an inverse relationship with *Prelp,* whereas *Ruminococcus torques* demonstrated a positive association with *mt-Nd5* and *Grem1*. Interestingly, *A. mucimiphila* displayed a strong negative correlation with proprotein convertase subtilisin/kexin type 9 (*Pcsk*9) (rho = − 0.94, $p = 0.016$), as well as weak negative corelation with *Ly6c*2 (rho = − 0.83, p = 0.058) and *Fcamr* (rho = − 0.37, $p = 0.50$) (Fig. 5b, Table S4). Collectively, these results highlight the complex interactions between the gut microorganisms and host gene expression.

Discussion

As a key physiological protein, osteopontin deficiency can exacerbate inflammatory reactions and damage intestinal health [14]. This study utilized an intestine-specific *Spp*1 conditional knockout mouse model to elucidate the coordinated role of OPN in regulating host gene expression and gut microbiota. *Spp*1 deletion resulted in a thinned colonic mucus layer and dysregulated expression of lipid metabolism or immune-related genes, such as *C*3, *Cdh*3, *Adora*1, *Pla2 g12b*, *Gcnt*3, and *Adra2a*. Besides, insufficient expression of endogenous OPN also lead to a marked reduction in mucin-dependent *A. muciniphila* abundance. These findings suggested that OPN maintains gut homeostasis through multifaceted mechanisms, including modulation of host gene expression, microbial metabolic pathways, and immune microenvironments.

While our data demonstrated correlations between gene expression and microbiota shifts in *Spp*1 conditional knockout mice, the directionality of causality remains unresolved. However, existing knowledge has shown that OPN affects intestinal immunity and barrier function through complex network regulation, which may occur through multiple pathways. On the one hand, host genes directly shaping microbial niches via mucus secretion or inflammatory cues, and abnormal expression of genes leads to disruption of immune balance. In this study, the upregulation of *C*3 and *Cdh*3 could be considered to be associated with enhanced immune and inflammatory responses [15, 16], while *Cdh*3 overexpression may compromise normal cell adhesion, weaken the gut barrier, and elicit inflammatory responses [17]. On the other hand, OPN may affect the integrity of the gut barrier through lipid metabolism pathways. For instance,

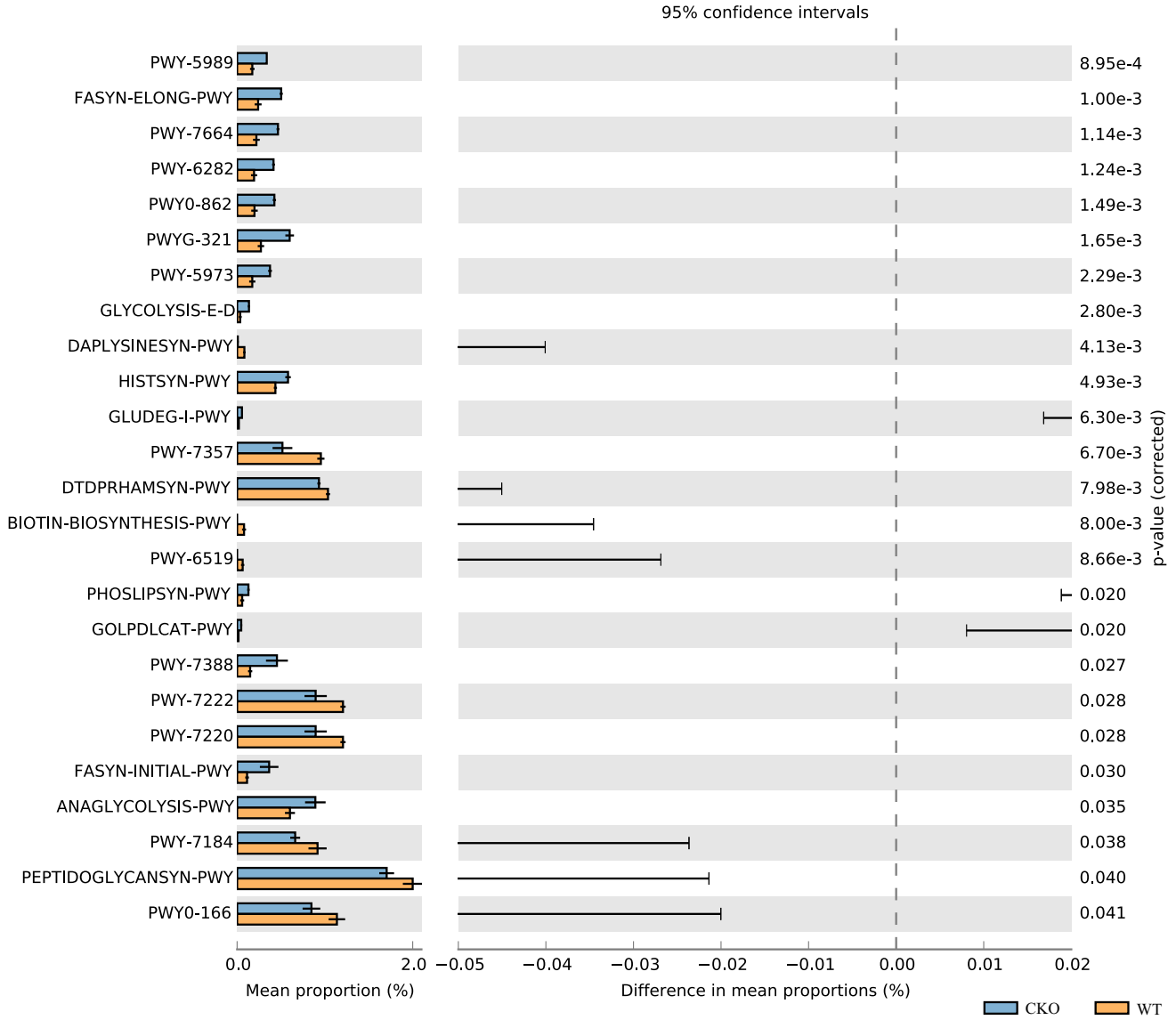

Fig. 4 Functional metabolic pathway analysis of gut microbiota. Based on KEGG database, functional metabolic pathways were predicted by HUMAnN2 (v3.6.0). The differential pathways between CKO (n = 3) and WT group (n = 3) were screened and visualized graphically by STAMP (v2.1.3) software. Benjamini Hochberg procedure was used for correction for testing, corrected $p < 0.05$ was considered statistically significant

the downregulation of *Gcnt*3 and *Pla2 g12b* was initially linked to lipid metabolism, and their roles may extend to epithelial integrity and glycosylation. *Gcnt*3, a glycosyltransferase critical for O-glycosylation of mucins, may compromise mucus layer glycoprotein structure and barrier function when suppressed [18]. Similarly, *Pla2 g12b*, a phospholipase A2 family member, could influence epithelial cell junctions via membrane phospholipid dynamics [19], suggesting that *Spp*1 conditional knockout disrupts intestinal barrier through multiple pathways (e.g., glycosylation defects, membrane instability).

Furthermore, our data support a hypothesized OPN-mediated positive feedback loop between *A. muciniphila* and the mucus layer. Specifically, OPN may sustain *A. muciniphila* colonization by maintaining mucus layer integrity, while mucin degradation by this bacterium generates metabolites such as SCFAs [20].These metabolites have been shown to stimulate goblet cell proliferation and enhance mucin secretion [21], thereby thickening the mucus layer and providing sustained carbon sources for *A. muciniphila*, establishing a self-reinforcing cycle [22, 23]. For instance, the concurrent reduction in mucus thickness and *A. muciniphila* abundance in *Spp*1 conditional

knockout mice suggests that OPN deficiency disrupts this loop. This mechanism not only explains *A. muciniphila*'s dependency on host mucins but also highlights OPN's dual role in regulating epithelial regeneration through microbial metabolites. Future studies should employ metabolomic profiling and goblet cell-specific conditional knockout models to directly validate causal links within this feedback system.

Numerous studies have highlighted the critical role of gut microbiota in regulating host health [24]. This microbiota–host relationship is highly symbiotic and characterized by mutual dependence. Gut microorganisms support host gut health by modulating immune responses, aiding metabolic functions, and protecting against pathogenic infections [25]. Conversely, genetic variations in the host can influence the composition of gut microbiota [26]. In this study, gene knockout altered the physiological state and gene expression of the host, leading to direct and indirect changes in the structure and function of the gut microbiota. It is worth considering whether changes in host gene expression drove alterations in the gut microbiota or whether changes in the gut microbiota caused differences in the host's gene expression. It was hypothesized that initial changes in host gene expression might have triggered the upregulation or downregulation of other genes, leading to physiological changes in the host that subsequently influence the composition and functionality of the gut microbiota. Alternatively, certain gene alterations could directly affect the gut microbiota, resulting in changes in microbial composition, inducing modifications in other host genes, and consequent physiological changes. This intricate and tightly connected interaction between the host and gut microbiota underscores the complexity of their relationship, and the specific mechanisms remain to be fully elucidated.

While this study elucidates the impact of intestine-specific *Spp*1 conditional knockout on host gene expression and gut microbiota, several limitations should be noted. First, the small sample size ($n = 3$ per group) was constrained by the rigorous littermate-controlled design (WT and CKO born from the same litter), sex-specific selection (male-only), and genetic homogeneity requirements. Although this design minimized confounding effects from genetic variability and early-life microbiota colonization, supporting the robustness of observed significant differences ($p < 0.05$, $|\log_2$ Fold Change$| > 1$), limited sample size may increase the risk of false negatives. Future studies will expand cohorts across multiple litters to enhance generalizability. Second, while focusing on two-month-old mice allowed us to capture early effects of *Spp*1 deletion, the study did not address outcomes in critical physiological stages (e.g., aging or lactation). For instance, lactating mice with hormonal and metabolic fluctuations may exhibit exacerbated gut barrier dysfunction, while chronic OPN deficiency in aged individuals could drive systemic inflammation or metabolic compensation. Follow-up investigations will systematically evaluate *Spp*1's roles across diverse age groups and physiological states to fully delineate its dynamic contributions to intestinal homeostasis.

Despite these limitations, our work provides critical evidence for OPN's central role in gut gene-microbiota crosstalk and proposes a framework for its regulation of homeostasis via immune-metabolic-microbial axes. Our findings highlight gut microbiota dysbiosis and metabolic perturbations in *Spp*1 conditional knockout mice, suggesting microbiome-targeted interventions (e.g., OPN supplementation or probiotics) as potential therapeutic strategies. For instance, exogenous OPN supplementation has been shown to restore mucus layer integrity and modulate immune microenvironments [27], while probiotic colonization (e.g., *Akkermansia muciniphila*) improves metabolic syndrome and mucosal barrier function [28, 29]. Future studies could explore the following: (1) OPN supplementation: Administering recombinant OPN protein (oral or intraperitoneal) to assess its ability to rescue mucus defects, gene expression, and microbiota composition in CKO mice; (2) Probiotic interventions: Supplementing *A. muciniphila* or its metabolites to determine if lipid metabolism and inflammatory phenotypes are reversed; (3) Utilizing germ-free mice or fecal microbiota transplantation (FMT) to dissect causal host-microbe interactions. For example, transplanting CKO microbiota into WT mice could test whether microbial shifts drive host phenotypes, and vice versa. These approaches would clarify OPN-microbiota mechanistic links and inform therapeutic strategies targeting gut ecosystems.

Conclusion

In this study, we revealed the significant impact of endogenous intestinal epithelial OPN deficiency on colonic polysaccharide mucus secretion, intestinal gene expression, and gut microbiota composition in two-month-old mice. The results demonstrate that intestine-specific *Spp*1 conditional knockout leads to reduced colonic polysaccharide mucus secretion, which may compromise the intestinal barrier function and further alter the composition and stability of the gut microbiota. Concurrently, the lack of OPN significantly alters the gene expression profiles related to immune regulation and lipid metabolism, highlighting the critical role of OPN in maintaining intestinal immune homeostasis and metabolic balance. Additionally, changes in the gut microbiota, particularly the reduction of beneficial bacteria such as *A. muciniphila*, may be closely associated with the thinning of the mucus layer and alterations in the intestinal environment induced by OPN deficiency. These findings underscore the essential role of endogenous intestinal epithelial OPN

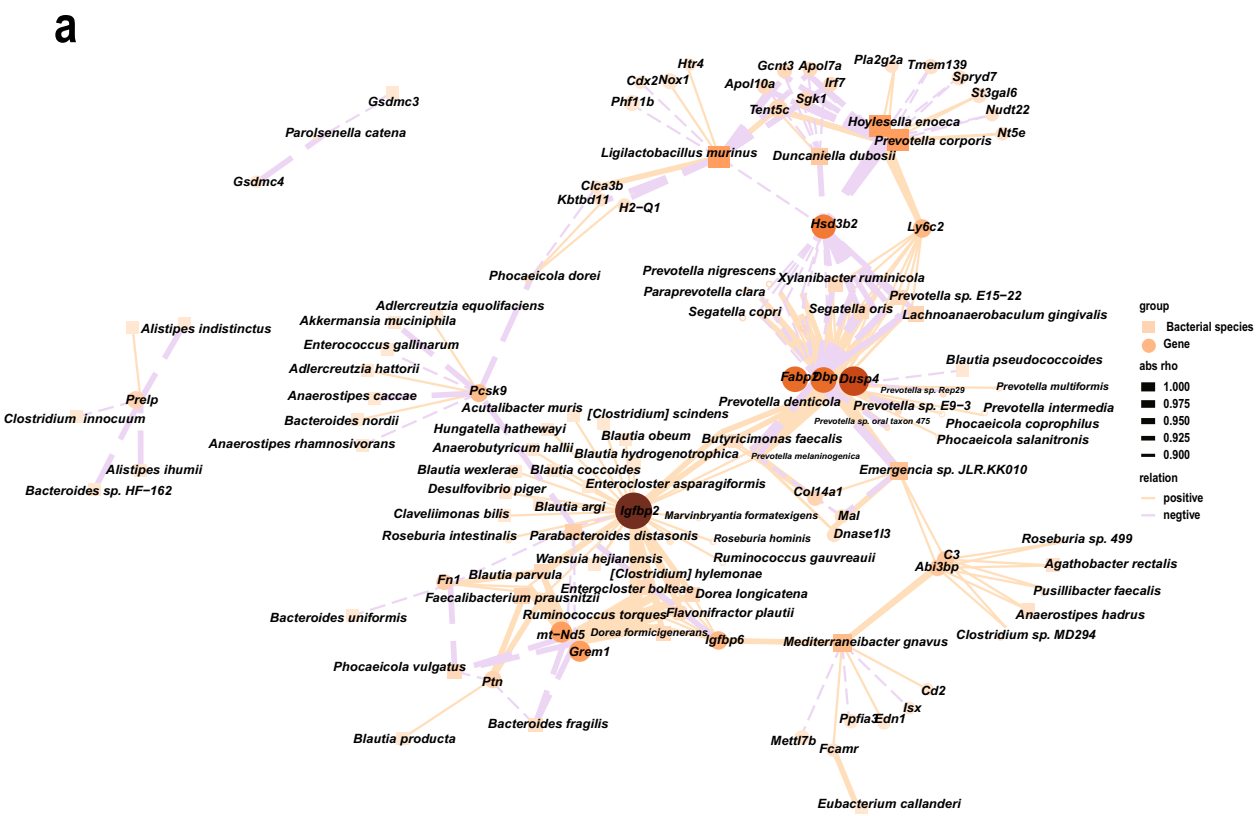
a
Htr4
Gcnt3
Apol7a
Pla2g2a
Tmem139
Spryd7
Cdx2
Nox1
Apol10a
Irf7
St3gal6
Phf11b
Tent5c
Sgk1
Nudt22
Gsdmc3
Hoylesella enoeca
Parolsenella catena
Prevotella corporis
Nt5e
Ligilactobacillus murinus
Duncaniella dubosii
Gsdmc4
Clca3b
Kbtbd11
H2−Q1
Hsd3b2
Ly6c2
Phocaeicola dorei
Prevotella nigrescens
Xylanibacter ruminicola
Paraprevotella clara
Prevotella sp. E15−22
Adlercreutzia equolifaciens
Segatella copri
Segatella oris
Lachnoanaerobaculum gingivalis
Alistipes indistinctus
Akkermansia muciniphila
Enterococcus gallinarum
Blautia pseudococcoides
Adlercreutzia hattorii
Fabp2
Dbp
Dusp4
Prevotella sp. Rep29
Prevotella multiformis
Prelp
Pcsk9
Anaerostipes caccae
Acutalibacter muris
[Clostridium] scindens
Prevotella denticola
Prevotella sp. E9−3
Prevotella intermedia
Clostridium innocuum
Bacteroides nordii
Prevotella sp. oral taxon 475
Phocaeicola coprophilus
Hungatella hathewayi
Blautia obeum
Butyricimonas faecalis
Anaerostipes rhamnosivorans
Anaerobutyricum hallii
Blautia hydrogenotrophica
Prevotella melaninogenica
Phocaeicola salanitronis
Alistipes ihumii
Blautia wexlerae
Blautia coccoides
Emergencia sp. JLR.KK010
Bacteroides sp. HF−162
Enterocloster asparagiformis
Desulfovibrio piger
Col14a1
Blautia argi
Igfbp2
Marvinbryantia formatexigens
Mal
Claveliimonas bilis
Dnase1l3
Roseburia intestinalis
Parabacteroides distasonis
Roseburia hominis
Roseburia sp. 499
Wansuia hejianensis
Ruminococcus gauvreauii
C3
Abi3bp
Agathobacter rectalis
Fn1
Blautia parvula
[Clostridium] hylemonae
Enterocloster bolteae
Dorea longicatena
Pusillibacter faecalis
Faecalibacterium prausnitzii
Bacteroides uniformis
Ruminococcus torques
Flavonifractor plautii
Anaerostipes hadrus
mt−Nd5
Dorea formicigenerans
Igfbp6
Mediterraneibacter gnavus
Clostridium sp. MD294
Grem1
Phocaeicola vulgatus
Ptn
Cd2
Isx
Ppfia3
Edn1
Bacteroides fragilis
Blautia producta
Mettl7b
Fcamr
Eubacterium callanderi
group
Bacterial species
Gene
abs rho
1.000
0.975
0.950
0.925
0.900
relation
positive
negtive
b
Pla2g2a
Hsd3b2
Gcnt3
Tmem139
Sgk1
Spryd7
Apol10a
Nudt22
Irf7
Igfbp6
Igfbp2
Nt5e
Tent5c
St3gal6
Apol7a
Gsdmc4
Mptx1
Ly6c2
Clca3b
Pcsk9
Mettl7b
Ahnak2
Edn1
Abi3bp
Kbtbd11
Akkermansia muciniphila
H2−Q1
Prelp
Isx
Itih2
Ppfia3
Enpp2
Dusp4
Fcamr
Cd2
Ptn
mt−Nd5
Mal
Fabp2
Dnase1l3
Cdx2
Gsdmc3
Fn1
Col14a1
C3
Phf11b
Nox1
Grem1
Dbp
Htr4
group
Gene
Bacterial species
abs_rho
0.8
0.6
0.4
0.2
relation
positive
negtive

◂**Fig. 5** Correlation network **a** Correlation network of gut microbiota and differential genes in CKO mice ($p < 0.05$, |rhol> 0.4). **b** Correlation between *Akkermansia muciniphila* and differentially expressed genes in CKO Mice. Solid lines represent positive correlations between species abundance and differentially expressed genes, whereas dashed lines represent negative correlations. The thickness of the lines indicates the strength of the correlation and the size and color of the points represent the number of correlated entities. Correlation analysis was conducted by multiple tests using Benjamini Hochberg FDR for calibration

in maintaining gut health and provide new insights into the potential mechanisms of OPN in intestinal diseases. Future studies could further explore the therapeutic potential of OPN in intestinal barrier repair and microbiota modulation.

Supplementary Information The online version contains supplementary material available at https://doi.org/10.1007/s00284-025-04246-6.

Acknowledgements This work was supported by the National Natural Science Foundation of China (32325040), Basic Research Operating Expenses Program for Colleges and Universities directly under the Inner Mongolia Autonomous Region (BR22–14–01), and the earmarked fund for CARS36. Nutrition and Care of Maternal & Child Research Fund Project" of Biostime Institute of Nutrition & Care-2022BINCMCF007.

Author Contributions Zhihong Sun, Yong Zhang, and Guangqi Gao conceived and designed the experiments. Na Li, Chunyan Zhao, Yue Zhao, and Tao Zhang conducted the experiments. Na Li analyzed the data. Na Li and Guangqi Gao drafted the manuscript. All authors have read and approved the final manuscript.

Data Availability The data in this study were uploaded to the BIG Submission database, and the BioProject ID number was PRJCA031775.

Declarations

Conflict of interest The authors declare no conflicts of interest.

References

1. Lin EY, Xi W, Aggarwal N, Shinohara ML (2023) Osteopontin (OPN)/SPP1: from its biochemistry to biological functions in the innate immune system and the central nervous system (CNS). Int Immunol 35(4):171–180
2. Wang L, Niu X (2024) Immunoregulatory roles of osteopontin in diseases. Nutrients 16(2):312
3. Bastos ACSDF, Gomes AVP, Silva GR, Emerenciano M, Ferreira LB, Gimba ERP (2023) The intracellular and secreted sides of osteopontin and their putative physiopathological roles. Int J Mol Sci 24(3):2942
4. Barkas GI, Kotsiou OS (2023) The role of osteopontin in respiratory health and disease. J Pers Med 13(8):18
5. Kumari A, Kashyap D, Garg VK (2024) Osteopontin in cancer. Adv Clin Chem 118:87–110
6. Rittling SR (2011) Osteopontin in macrophage function. Expert Rev Mol Med 13(19):e15
7. Shinohara ML, Lu L, Bu J, Werneck MBF, Kobayashi KS, Glimcher LH, Cantor H (2006) Osteopontin expression is essential for interferon-alpha production by plasmacytoid dendritic cells. Nat Immunol 7(5):498–506
8. Li L, Chen J, Zheng Y, Lane J, Hu R, Zhu J, Fu X, Huang Q, Liu F, Zhang B (2024) Gastro-intestinal digested bovine milk osteopontin modulates gut barrier biomarkers in vitro. Mol Nutr Food Res 68(4):e2200777
9. Levy E, Marcil V, Tagharist Ep Baumel S, Dahan N, Delvin E, Spahis S (2023) Lactoferrin, osteopontin and lactoferrin-osteopontin complex: a critical look on their role in perinatal period and cardiometabolic disorders. Nutrients 15(6):1394
10. Sorensen ES, Christensen B (2023) Milk osteopontin and human health. Nutrients 15(11):2423
11. Xi M, Liang D, Yan Y, Duan S, Leng H, Yang H, Shi X, Na X, Yang Y, Yang C et al (2023) Functional proteins in breast milk and their correlation with the development of the infant gut microbiota: a study of mother-infant pairs. Front Microbiol 14:1239501
12. Church DM, Schneider VA, Graves T, Auger K, Cunningham F, Bouk N, Chen HC, Agarwala R, Mclaren WM, Ritchie GR (2011) Modernizing reference genome assemblies. PLoS Biol 9(7):e1001091
13. Wood DE, Lu J, Langmead B (2019) Improved metagenomic analysis with Kraken 2. Genome Biol 20(1):257
14. Woo SH, Lee SH, Park JW, Go DM, Kim DY (2019) Osteopontin protects colonic mucosa from dextran sodium sulfate-induced acute colitis in mice by regulating junctional distribution of occludin. Dig Dis Sci 64(2):421–431
15. Sugihara T, Kobori A, Imaeda H, Tsujikawa T, Amagase K, Takeuchi K, Fujiyama Y, Andoh A (2010) The increased mucosal mRNA expressions of complement C3 and interleukin-17 in inflammatory bowel disease. Clin Exp Immunol 160(3):386–393
16. Scott D, Botto M (2016) The paradoxical roles of C1q and C3 in autoimmunity. Immunobiology 221(6):719–725
17. Hsiao TF, Wang CL, Wu YC, Feng HP, Chiu YC, Lin HY, Liu KJ, Chang GC, Chien KY, Yu JS et al (2020) Integrative omics analysis reveals soluble cadherin-3 as a survival predictor and an early monitoring marker of EGFR tyrosine kinase inhibitor therapy in lung cancer. Clin Cancer Res Off J Am Assoc Cancer Res 26(13):3220–3229
18. Rinaldi M, Dreesen L, Hoorens PR, Li RW, Claerebout E, Goddeeris B, Vercruysse J, Van Den Broek W, Geldhof P (2011) Infection with the gastrointestinal nematode *Ostertagia ostertagi* in cattle affects mucus biosynthesis in the abomasum. Vet Res 42(1):61

19. Le May C, Ducheix S, Cariou B, Rimbert A (2025) From genetic findings to new intestinal molecular targets in lipid metabolism. Curr Atheroscler Rep 27(1):26
20. Mei L, Wang J, Hao Y, Zeng X, Yang Y, Wu Z, Ji Y (2024) A comprehensive update on the immunoregulatory mechanisms of Akkermansia muciniphila: insights into active ingredients, metabolites, and nutrient-driven modulation. Crit Rev Food Sci Nutr 1-18
21. Ambat A, Antony L, Maji A, Ghimire S, Mattiello S, Kashyap PC, More S, Sebastian V, Scaria J (2024) Enhancing recovery from gut microbiome dysbiosis and alleviating DSS-induced colitis in mice with a consortium of rare short-chain fatty acid-producing bacteria. Gut Microb 16(1):2382324
22. Davey LE, Malkus PN, Villa M, Dolat L, Holmes ZC, Letourneau J, Ansaldo E, David LA, Barton GM, Valdivia RH (2023) A genetic system for *Akkermansia muciniphila* reveals a role for mucin foraging in gut colonization and host sterol biosynthesis gene expression. Nat Microbiol 8(8):1450–1467
23. Kim S, Shin YC, Kim TY, Kim Y, Lee YS, Lee SH, Kim MN (2021) Mucin degrader *Akkermansia muciniphila* accelerates intestinal stem cell-mediated epithelial development. Gut Microb 13(1):1–20
24. Heintz-Buschart A, Wilmes P (2018) Human gut microbiome: function matters. Trends Microbiol 26(7):563–574
25. Hooper LV, Littman DR, Macpherson AJ (2012) Interactions between the microbiota and the immune system. Science 336:1268
26. Goodrich JK, Waters JL, Poole AC, Sutter JL, Koren O, Blekhman R, Beaumont M, Van Treuren W, Knight R, Bell JT et al (2014) Human genetics shape the gut microbiome. Cell 159(4):789–799
27. Han L, Li Q, Du M, Mao X (2024) Bovine milk osteopontin improved intestinal health of pregnant rats fed a high-fat diet through improving bile acid metabolism. J Dairy Sci 107(1):24–39
28. Plovier H, Everard A, Druart C, Depommier C, Van Hul M, Geurts L, Chilloux J, Ottman N, Duparc T, Lichtenstein L et al (2017) A purified membrane protein from *Akkermansia muciniphila* or the pasteurized bacterium improves metabolism in obese and diabetic mice. Nat Med 23(1):107–113
29. Zheng M, Han R, Yuan Y, Xing Y, Zhang W, Sun Z, Liu Y, Li J, Mao T (2022) The role of *Akkermansia muciniphila* in inflammatory bowel disease: current knowledge and perspectives. Front Immunol 13:1089600